Particle Beam-Induced Reactions versus Thermal Degradation in PMDA–ODA Polyimide

Giovanni Marletta*

Dipartimento di Scienze Chimiche, Università di Catania, Viale A. Doria 6, 95125 Catania, Italy

Fabio Iacona

CNR, Istituto di Metodologie e Tecnologie per la Microelettronica, Viale A. Doria 6, 95125 Catania, Italy

Andras Toth

Research Laboratory for Inorganic Chemistry, Hungarian Academy of Sciences, Budaörsi út 45, H-1112, Budapest, Hungary

Received July 29, 1991; Revised Manuscript Received January 4, 1992

ABSTRACT: Chemical reactions induced by heat and particle bombardment at low energy in PMDA–ODA have been studied by XPS and REELS. Different chemical reactions involving the chemical state of oxygen and nitrogen are shown to occur with different products and rates depending on the peculiar way of energy deposition. In particular, thermal treatments proceed mainly by decarbonylation of imidic rings, leaving the ether linkage in the PMDA–ODA unit essentially unaffected. Evidence is found that thermal treatment results in the formation of large condensed aromatic systems, possible precursors for true graphitization at higher temperature. Also, a characteristic REELS signature is observed, diagnostic of the formation of a hydrogenated amorphous carbon phase. In the case of particle bombardment, the destruction of imide and phenyl rings occurs through a random fragmentation mechanism, leaving a detectable concentration of the imidic moiety at the steady state. A specific reaction channel has been identified, involving the production of recoiling oxygen atoms, which react with the carbon backbone to form new additional ether or hydroxyl groups. Also the electronic structure of the irradiated samples is shown to be different from that of the pyrolyzed samples. In particular, no evidence is found for the formation of large delocalized aromatic systems observed in the thermal case, while the predominant effect is the formation of highly disordered a-C:H phases.

Introduction

Ion bombardment of organic materials and particularly of polymers has been widely investigated in the last few years, in connection with the possibility of obtaining interesting modifications of their basic physical and chemical properties.[1–3] These have been shown to depend upon a number of parameters including ion energy and fluence, i.e., the total deposited energy per unit volume, and the predominant energy deposition mechanism.[4,5]

However, the connection between ion-induced chemistry and the fundamental ion–solid interaction events as well as the structural evolution of the bombarded phases and the basic modification mechanisms is not yet understood. As an example, we recall that ion-induced processes in polymers are often discussed in terms of "carbonization" or "graphitization" of the target,[3] supporting the idea that the ion–polymer interaction essentially is equivalent to some kind of violent thermal process.[6,7] At variance with this picture, in recent papers we demonstrated that the structure of the polymer under ion bombardment is continuously evolving toward a state that can be characterized as a hydrogenated amorphous carbon. During this evolution the chemical functionalities are modified, producing new definite chemical bonds, still depending on the initial composition of the polymer.[2]

One of the relevant problems when dealing with "fragile" objects like polymers is the basic nature of the ion-induced chemical reactions. In particular, it is not yet clear if the ion-induced process should be considered just equivalent or if it is intrinsically different from the "conventional" heat-induced ones. In the first case the emphasis is put on the very high deposition rate in the ion track. In the second case, the very specific nature of the energy deposition mechanisms is emphasized. In line with this view, in several recent papers we investigated the different chemical modifications induced by particle beams depositing energy mainly by electronic interaction or by binary collisions. Our results suggested that different energy deposition mechanisms induce different types of reactions.[2,8–10]

The aim of the present paper is to study the chemical products obtained with a typical ion bombardment experiment and those obtained in a classical heat-induced degradation of a model polymer. It is noted that the role of trivial thermal effects due to beam-induced heating should be distinguished from the effects of high-energy deposition rate, referred to as "electronic heating".[3] In order to avoid the overlap of the two effects, in this study the attention has been focused on a heat-resistant polymer, poly(*N*,*N*′-(*p*,*p*′-oxydiphenylene)pyromellitimide) (hereinafter indicated as PMDA–ODA), also known as Kapton. This polymer is resistant to heat-induced decomposition up to temperatures to the order of 400 °C, so preventing possible effects coming just from trivial beam-induced heating. Furthermore, both the thermal degradation and the ion-induced effects in polyimide have been widely studied and characterized by several techniques, including XPS, IR, FTIR, optical absorption, RBS, etc.,[11–22] so providing a large literature body with which to compare the present experimental data.

The present work is based on the use of XPS (X-ray photoelectron spectroscopy) and REELS (reflection electron energy loss spectroscopy) techniques to characterize the chemical changes produced in PMDA–ODA samples. Due to the fact that ion-bombarded surfaces of polymers are known to be very sensitive (depending on the projectile fluence) to exposure to the atmosphere, the irradiation treatments have been performed using a low-energy source

0024-9297/92/2225-3190$03.00/0

Table I
Elemental Composition Obtained by XPS of Bombarded and Thermally-Treated PMDA–ODA Samples

5-keV Ar^0				thermally treated			
dose	% C	% O	% N	T, °C (time, min)	% C	% O	% N
untreated	76.9	16.6	6.5	untreated	76.5	16.9	6.6
4.7×10^{13}	78.2	15.7	6.1	377 (50)	79.9	13.9	6.2
2.35×10^{14}	83.9	9.9	6.2	547 (72)	86.2	7.7	6.1
4.7×10^{14}	86.8	8.0	5.2	617 (81)	88.9	6.0	5.2
9.4×10^{14}	89.9	5.8	4.3	727 (95.6)	91.8	4.6	3.7
1.4×10^{16}	93.8	3.2	3.0	927 (122)	93.0	4.0	3.1

fitted to the XPS apparatus, to avoid any exposure of the sample surface to the atmosphere. For the same reason, the thermal treatments were performed in an Ar atmosphere and the samples were extracted from the oven only after cooling in inert atmosphere.

Experimental Section

Thin films of PMDA–ODA were obtained by spinning a solution of polyamic acid in *N*-methylpyrrolidone at a suitable dilution (Pyralin 2545 from E.I. du Pont de Nemours and Co.) at 5000 rpm for 45 s onto 5-in. Si wafers. The wafers were heated at 90 °C for 30 min in air to drive off the solvent, and therefore the polyamic acid film was imidized according to the procedure of ref 14a. The complete imidization was monitored by means of IR and XPS analyses. The typical thickness of the PMDA–ODA films obtained in this way was about 9000 ± 500 Å, as measured with an Alpha-Step apparatus (Tencor Instruments).

XPS and REELS analyses were performed using a Kratos ES 300 electron spectrometer, equipped with a Kratos electron gun, for REELS spectroscopy, operating with 50–5000-eV electron beams at variable currents (between 100 nA and 100 μA). The XPS take-off angle was 15°. The angle of incidence of the electron beam in the REELS experiments was 45° with respect to the normal to the sample surface positioned parallel to the analyzer's entrance slits.

The bombardment was performed in situ in the preparation chamber fitted to the XPS apparatus using an 11NF FAB source (from Ion Tech Ltd.) operating at 1–10 keV of noble gas atom beams with an incidence angle of 30° with respect to the normal to the sample surface. The particle currents were estimated by measuring the steady-state current due to the emission of secondary electrons and charged particles on a Cu target of known area and considering an ionization cross section on the order of 0.5, according to literature data.[23] The estimated current was 5.5 $\mu A/cm^2$ for 5 keV Ar^0 with a residual pressure of Ar of 6×10^{-5} Torr.

The XPS spectra were calibrated to the low binding energy (BE) component of the C 1s peak of PMDA–ODA assumed at 285.0 eV of BE before irradiation and pyrolysis.

The irradiation as well as the pyrolysis generally resulted in a shift of all the peaks of about 2.0 eV for particle bombarded samples and about 2.3 eV for heat-treated samples toward higher kinetic energies (KEs), implying a substantial increase in the electrical conductivity of the modified surfaces. Therefore, after treatments the referencing was performed by putting a gold sheet in electrical contact with the samples and taking the Au $4f_{7/2}$ peak at 83.8 eV.

Results and Discussion

Among the various types of heat- or radiation-induced chemical effects we will consider those consisting of compositional modifications, properly involving the variation of elemental ratios (Section 1), and chemical modifications of the primary structure, mainly involving the variation in the chemical state of oxygen and nitrogen (Sections 2 and 3) and the backbone structure (Section 4).

A preliminary point to be discussed concerns the homogeneity within the XPS and REELS sampling depth of heat- and irradiation-modified samples. The evaluated sampling depth for the C 1s photoelectrons (for Al Kα photons at 1486.6 eV) is about 85 Å and slightly less for N 1s and O 1s photoelectrons.[24] The same holds for electrons of comparable energy in REELS experiments (see Section 4). This thickness is lower than the mean projected range (about 100 Å) and the total range (about 123 Å) of Ar 5-keV projectiles as evaluated by TRIM code.[25] Furthermore, there is not a significant variation of the energy deposition mechanism along the track for the Ar 5-keV particles; i.e., the collisional term is the predominant one.[25] These two facts make us confident that the modification of the irradiated layer can be considered substantially homogeneous within the XPS and REELS sampling depth. On the other hand, no significant depth dependence of the surface composition is expected in the case of heat treatments, at least within the thickness relevant for XPS and REELS measurements.

However, the occurrence of different chemical reactions for particle irradiation, related to the variation in the energy deposition mechanism,[2,4,8–10] as well as the possibility of near-surface cage-type effects, also for thermal treatments, suggests the need for angular-dependent XPS studies to clarify the problem of the homogeneity of heat- or irradiation-induced surface modifications (outer 100 Å).

(1) Compositional Modification. Let us consider first the trends of compositional modification induced respectively by particle beams and thermal treatments.

Table I reports the data obtained by XPS analysis for PMDA–ODA bombarded with Ar^0 5-keV particles and the same polymer thermally treated.

The trend of compositional modification for 5-keV Ar^0 is very similar to the experiments performed using ions of similar energy.[17,21,22] In particular, the XPS signals of oxygen and nitrogen decrease for increasing particle fluence. Oxygen is more sensitive to depletion than nitrogen, the estimated elemental percentage being reduced from 16.6% to 3.2% in the sample bombarded at the highest dose (1.4×10^{16} Ar^0/cm^2), while the corresponding decrease of nitrogen ranges from 6.5% to 3.0%. In particular, it is noteworthy that the depletion trend of the N atoms is a very slow process (on the fluence scale), and no saturation point is observed, at least in the fluence range studied here. This behavior contrasts with the idea that ion-beam-induced carbonization is a violent process, leading essentially to a graphitelike phase losing any memory of its initial chemical structure.[3] The data in Table I in no way suggest that such a drastic process is occurring during ion bombardment. In fact, we can observe as much as 65% of the initial N at the polymer surface after a bombardment fluence of 1×10^{15} Ar^0/cm^2, when the chemical structure of the polymer and its physical properties are completely changed.[2]

It is also important to realize that the fluence dependence of the compositional modifications in our experiment (low-energy particles) is very close to the fluence dependence observed for bombardment with high-energy ions (more than 100 keV) on respectively PMDA–ODA[6,15,16,18] and BTDA–ODA.[14]

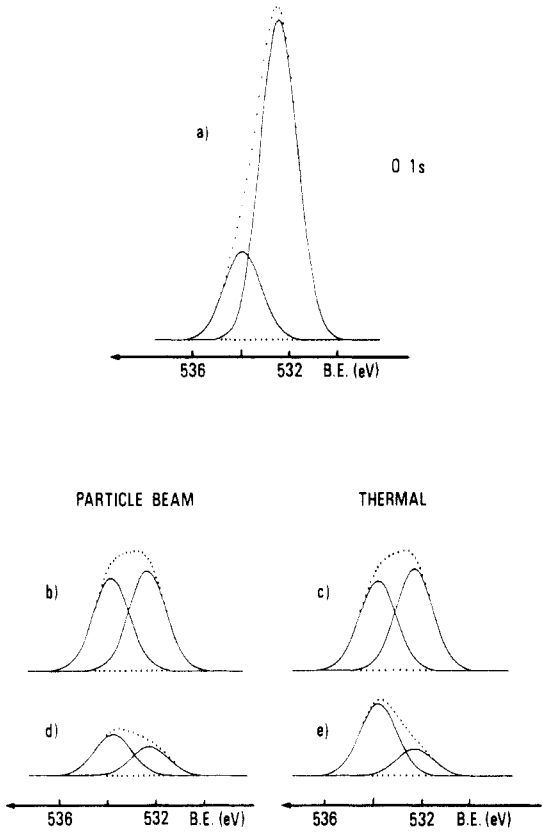

Figure 1. O 1s XPS peaks for PMDA–ODA: (a) untreated; (b) bombarded with 4.7×10^{14} Ar^0 5 keV/cm^2; (c) heated at 547 °C for 72 min; (d) bombarded with 1.4×10^{16} Ar^0 5 keV/cm^2; (e) heated at 927 °C for 122 min.

The heat-treated samples (Table I) show very similar qualitative and quantitative trends of compositional modification with respect to particle-irradiation effects. In particular, the composition of the samples treated at temperatures higher than 600 °C closely resembles that of samples bombarded at a fluence higher than 5×10^{14} particles/cm^2. Also the composition at the highest temperature we used in this experiment is very close to that obtained for the samples bombarded at the highest fluence 1.4×10^{16} Ar^0/cm^2.

On the basis of the data reported in Table I, we conclude that heat-treated and particle-bombarded samples show a common compositional modification trend, which does not allow us to distinguish between different chemical processes for the heat- and beam-induced modification of PMDA–ODA.

(2) Chemical Modifications of the Primary Structure. A preliminary comment is needed about the comparison between thermally-treated and Ar-irradiated samples. A correct comparison should be performed considering the chemical structure of samples in which equal amounts of energy have been deposited by respectively heating or particle bombardment. Due to the fact that it is very difficult to evaluate correctly these amounts of deposited energy in such different conditions of energy deposition, we will compare directly the chemical structure of samples having very similar elemental compositions, arguing that any differences in the chemical structure of compositionally similar samples are indicative of different chemical processes.

In particular, the samples irradiated at 4.7×10^{14}, 9.4×10^{14}, and 1.4×10^{16} Ar^0/cm^2 and samples respectively treated at 547 °C (for 72 min), 727 °C (for 81 min), and 927 °C (for 122 min) have very similar compositions and can be considered in parallel two by two. Figure 1 reports the characteristic modification trend of the O 1s peak for untreated, particle-bombarded, and heat-treated samples of comparable composition.

According to a well-established literature, the O 1s peak for PMDA–ODA has been analyzed in terms of two bands respectively assigned to the imide carbonyl (at 532.3 eV) and to the ether linkage (at 533.8 eV). The thermal treatment as well as the particle bombardment does not change the BE of the two O 1s components. However, it should be recalled that the real chemical nature of the groups contributing to the O 1s bands after thermal or particle beam treatments is not unequivocally assigned with respect to the untreated polymer. In fact, it is well-known that the oxygen atoms belonging to several types of chemical groups like phenolic and alcoholic hydroxyls, esters, and ethers fall in the BE region around 533.0–533.8 eV, and many types of C=O-containing groups give a peak around 532.0–532.5 eV of BE.[26,27] Therefore, we will indicate the component at 533.8 eV in bombarded and thermally-treated samples as "ether-like", keeping in mind that also hydroxyl groups can be present.

The expected stoichiometry of carbonyl-to-ether components for untreated PMDA–ODA is 4:1 versus an experimental ratio of 3.6:1, showing the well-known and widely reported small deficiency in the carbonyl content which has been generally found from XPS studies of the surface of fully cured polyimides.[28,29] Both heat treatments and particle bombardment produce the modification of this characteristic ratio, mainly seen as a strong depletion of the carbonylic component. This effect has been explained in terms of imide ring degradation and related molecular rearrangements starting with the loss of the carbonyl groups, while the apparent stability of the intensity of the ether-like band has been attributed to the high radiation resistance of the ether linkage, stabilized by the two contiguous benzene rings. The effect seems qualitatively very similar, but quantitative differences are seen for the two types of treatments.

We remark that while in general only the *relative* decrease of the carbonyl component with respect to the ether-like component of the O 1s band has been reported,[11-13,15-18,20-22] in the present experiment we focused our attention on the determination of the *absolute* concentration trends of the two different types of oxygen. In particular, parts a and b of Figure 2 report the absolute quantitative modification, with thermal or particle treatments, of the percentage of carbonylic or ether-like oxygens with respect to the initial total oxygen (see Table I).

In particular, Figure 2a shows for heated samples a steep decrease of the carbonyl concentration from 78% to 7% of the initial total oxygen content. This corresponds to a decrease from 13.2% to 1.1% as a percent of the total number of atoms (i.e., C, N, and O) excluding H atoms. On the other hand, the ether-like component undergoes a very small total decrease from 22% to 17% of the total initial oxygen corresponding to a decrease from 3.7% to 2.9% as a percent of the total atoms (see above). Therefore, the total decrease of oxygen in heated samples is due essentially to the preferential depletion of C=O groups, while the higher expected stability of the ether linkage is confirmed.

In the particle-bombarded samples (Figure 2b) the modification trend of the oxygen content is very different. In fact, the continuous decrease of the carbonyl-like component is initially balanced by the absolute increase (roughly a factor of 2) of the ether-like component at low fluence (up to 5×10^{13} Ar^0/cm^2). At this fluence there is

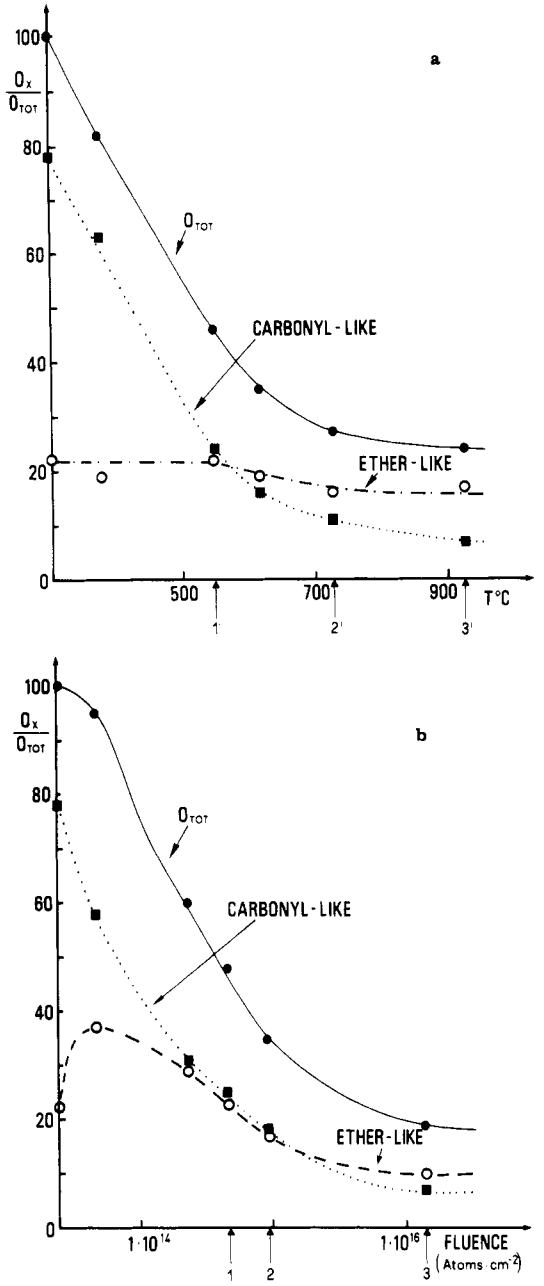

Figure 2. Percent variation of the total oxygen and related functional groups: (a) thermally-induced traces; (b) bombardment-induced traces. The arrows refer to samples of comparable elemental composition.

a very small loss of total oxygen, suggesting that carbonylic oxygen is transformed in the ether-like one. This unexpected increase is then followed by a slow depletion at higher fluence. The final concentration of the ether-like oxygen, with respect to the initial total oxygen content, is lower in the case of Ar irradiation (10%, i.e., 1.7% of the total number of atoms) than in the case of thermal treatments (17%, i.e., 2.9% of the total number of atoms). This fact suggests that the particle irradiation is finally more effective in depleting the ether-type oxygen.

The N 1s band shows a complex pattern of modification, with the creation of new components corresponding to the formation of different chemical states of nitrogen. Figure 3 shows N 1s bands for heat-treated and particle-bombarded samples of comparable composition.

The band shape for the virgin samples (Figure 3a) according to the literature[28,29] and previous results from this laboratory[10,14,30] is resolved into two bands respectively assigned to the imidic ring nitrogen (at 400.8 eV) and to a small quantity of isoimide (at 399.3 eV), always present

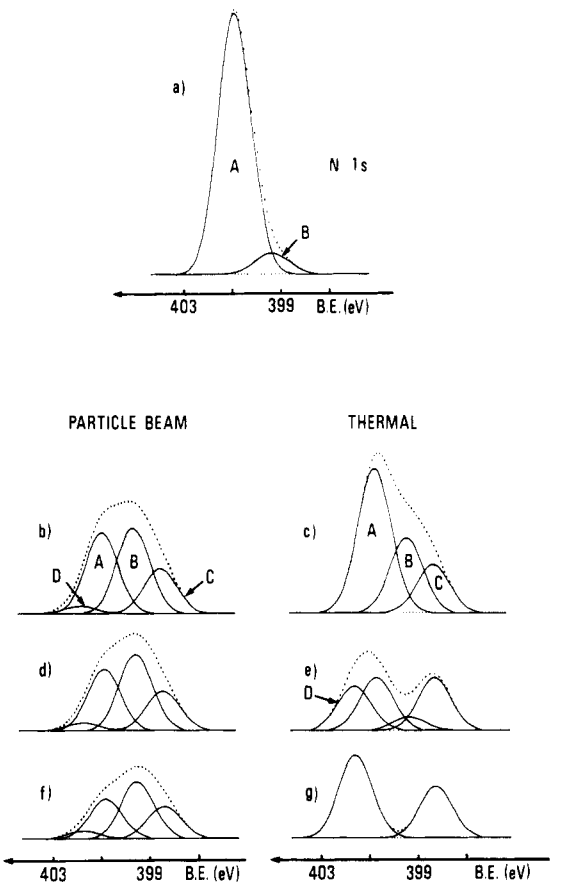

Figure 3. N 1s XPS peaks for PMDA-ODA: (a) untreated; (b) bombarded with 4.7×10^{14} Ar^0 5 keV/cm^2; (c) heated at 547 °C for 72 min; (d) bombarded with 9.4×10^{14} Ar^0 5 keV/cm^2; (e) heated at 727 °C for 95.6 min; (f) bombarded with 1.4×10^{16} Ar^0 5 keV/cm^2; (g) heated at 927 °C for 122 min.

after thermal curing in polyimides.[28,29]

The thermal treatment (see Figure 3c,e,g) essentially decreases the intensity of the imidic band (component A) and produces the transient increase of the band at 399.3 eV (component B), also creating two new bands respectively at 398.6 eV (component C) and 401.4 eV (component D). At the highest temperature only these new bands (components C and D) remain in the pyrolyzed samples.

According to Toth et al.,[12] we assign the band at 399.3 eV (component B) after thermal treatment to the formation of linear =C=N— linkages (imine group) or to nitrile groups —C≡N, which are expected to fall in the same BE range. The formation of both such groups is expected for thermal degradation, involving the rupture of the imide ring and its rearrangement.[31,32]

Component C at 398.6 eV is assigned to pyridine-type nitrogen present in aromatic rings produced during thermally-induced condensation processes, according to several authors.[32] This assignment is also supported by previous measurements in our laboratory on poly(2-vinylpyridine) and poly(4-vinylpyridine) yielding a BE for nitrogen in isolated aromatic rings of 398.8–398.9 eV, very close to the present result.

More difficult is the assignment of component D at 401.4 eV in heat-treated samples. A previously proposed assignment to amide-like groups contrasts with the fact that the BE of the -NH group in PMDA-ODA parent polyamic acid is found at 400.4 eV. On the other hand, literature reports assign a BE of 401.4 eV to a quaternary nitrogen group[33] or to a tertiary amine moiety.[34] Evidence for the formation of quaternary nitrogen in PMDA-ODA has been claimed in high energy electron irradiation

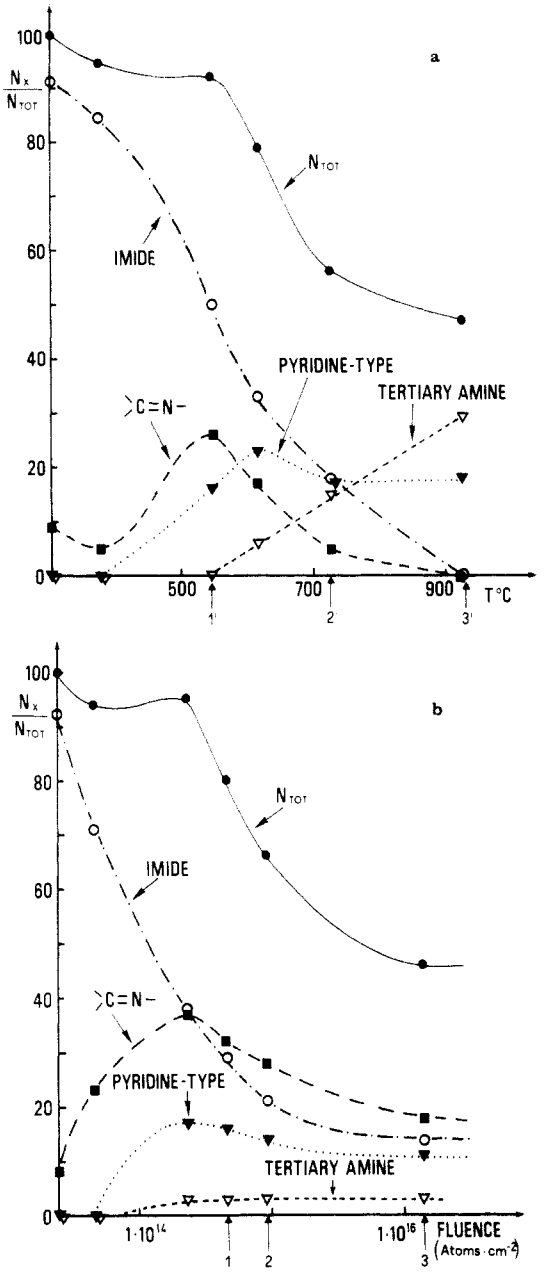

Figure 4. Percent variation of the total nitrogen and related functional groups: (a) thermally-induced traces; (b) bombardment-induced traces. The arrows refer to samples of comparable elemental composition.

experiments,[35] but this species should be very unstable, so that we suggest that 401.4-eV band is due to tertiary nitrogen groups, probably enclosed in condensed cycles.

The absolute quantitative trends for thermally-treated samples are reported in Figure 4a in terms of the initial total nitrogen content. The monotonic disappearance of the imide component is accompanied by a transient increase of the imine group concentration, followed by its complete depletion with the delayed formation of the component attributed to tertiary amine, which starts to be formed when the concentration of the imine is at its maximum. This behavior recalls the kinetics of a consecutive reaction, in which the imine groups, starting at a critical concentration, are progressively transformed in (cyclic) tertiary nitrogen groups. Furthermore, we may observe the growth of the pyridine-like component reaching a steady state, so that the final state composition for N-containing groups consists of these pyridine-like groups and tertiary nitrogen.

Scheme I

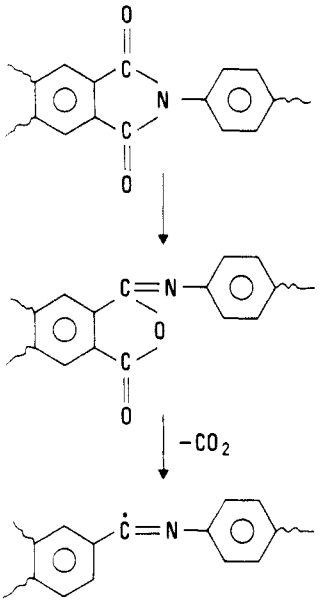

In the case of Ar-irradiated samples (Figure 3b,d,f) the modification pattern is quite different. In particular, the imide band (component A in Figure 3, falling at 400.7 eV after bombardment) is still present at the steady state while the imine component at 399.3 eV becomes the most intense of the pattern (with a small transient increase around 1×10^{14} and 5×10^{14} Ar^0/cm^2). It should be noted that the band at 400.7 eV in bombarded samples could contain a small contribution from amide groups, expected at 400.4 eV[14,28] and close enough to the imide band to be seen as a unique component.

As to the new components, a pyridine-like band is observed also in this case with an appreciable intensity, but the tertiary nitrogen component at 401.4 eV is of negligible intensity through all the particle bombardment. The whole process of nitrogen conversion, as summarized in Figure 4b, therefore consists of the parallel, simultaneous increase of the linear =C=N— and pyridine-like components at the expense of the imide nitrogen, which is not completely depleted.

(3) Chemical Mechanisms. Comparison of parts a and b of Figure 2 allows the identification of two main chemical processes related to the oxygen-containing functionalities.

The first consists of the rupture of imidic rings via the *elimination* of carbonyl groups, either through an isomerization and decarboxylation mechanism (see Scheme I) yielding a residual imine group or through the process summarized in Scheme II, producing a residual nitrile. These mechanisms seem to operate for thermal as well as particle bombardment treatments.

The second process, observed here for the first time, is characteristic of particle bombardment treatments. It produces the transient increase of the ether- or hydroxyl-like groups at the expense of the carbonyl groups (Scheme III). This peculiar pathway of production of ether- or hydroxyl-like groups can be understood in terms of the *transformation* of the carbonyl groups due to the collisional breaking of these groups, producing recoiling free oxygen species (radicals or hot atoms) available for reactions with suitable carbon sites. The proposed chemical effect is in part similar to that reported for the bombardment of PMDA–ODA directly with low-energy O_2 ions (O_2–RIBE), where the formation of both C–O and C=O groups was observed.[36]

Scheme II

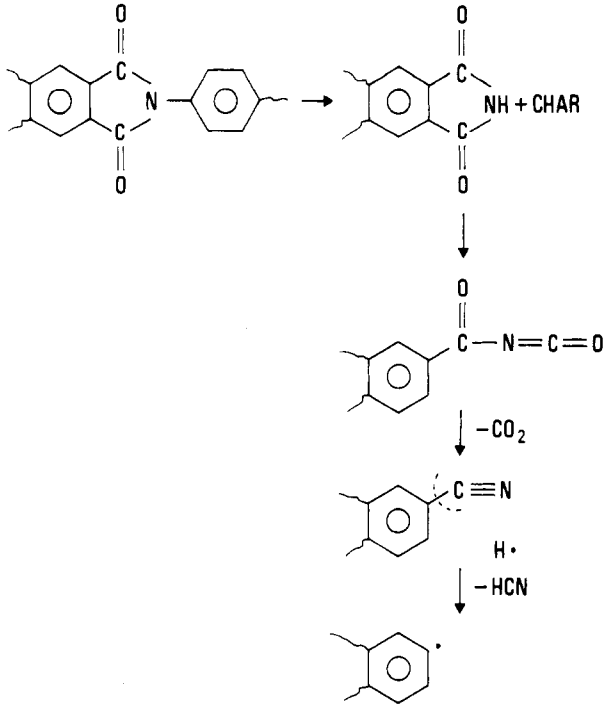

Scheme III

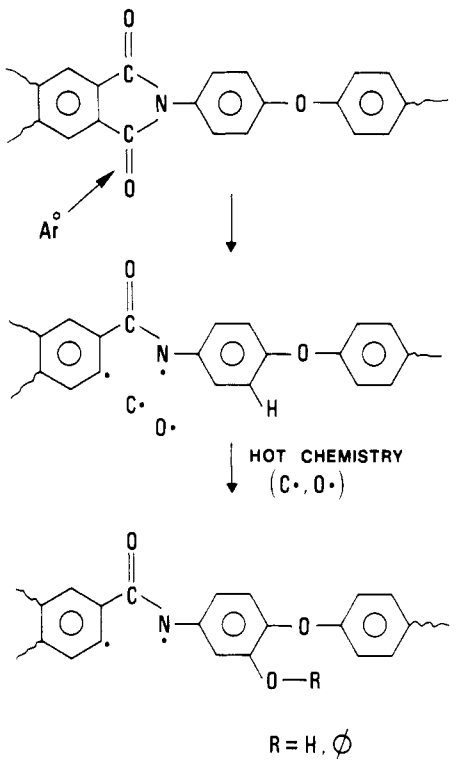

Such a mechanism is characteristic of particle-beam-induced chemistry, and therefore it should not be observed for the heat-induced chemistry, as is shown in the present experiment, as well as in electronic energy deposition processes. In agreement with this hypothesis, irradiation of PMDA–ODA samples with 3-keV electrons (i.e., not involving collisional energy deposition) does not induce any transient formation of ether- or hydroxyl-like groups.[10]

The peculiar increase of highly reactive ether- or hydroxyl-like oxygen sites is expected to enhance the reactivity of the beam-bombarded surfaces as compared to the virgin or the pyrolyzed surfaces. In this respect it is interesting to note that the increase of the ether (or hydroxyl) band is observed in the fluence range 10^{14} particles/cm^2, while at higher fluence, this new oxygen species is sputtered away with a slowly decreasing tail, suggesting a balance between the production of new ether-like groups and the rate of sputtering. In the same fluence range around 10^{14} particles/cm^2 some authors find a definite improvement of the adhesion performances of PMDA–ODA–metal layers under keV ion beam irradiation, which degrades at higher ion fluence.[37] Therefore, our finding provides a chemical basis for explaining the observed adhesion improvement following low-energy bombardment of PMDA–ODA in terms of the increase of reactive oxygen sites available for bonding with metal atoms at the bombarded surfaces.[22,37,38]

In the case of nitrogen-containing groups, the thermally-induced modifications are characterized by a consecutive reaction producing a transient increase of the imine-like concentration followed by the transformation of this group in some kind of cyclic tertiary amine and an apparently independent process of transformation of the imide groups in pyridine-type structures (see Figure 4a).

At variance with this, in the case of particle-bombarded samples, the three reactions are observed to occur almost simultaneously, with different growth rates (see Figure 4b). This seems characteristic of specific beam-related processes, mainly based on the fact that all the precursor states are simultaneously produced due to the very high energy input due to the collisional processes as well as the random nature of the particle-induced bond breaking.

The above-described reactions of decarbonylation (Schemes I and II) account for the observed production of the imine groups as intermediates of thermal- and particle-induced reactions. Trends in Figure 4a suggest that the reaction of formation of tertiary amine groups may start from such an imine intermediate, but the mechanism of formation of tertiary amine also needs the presence of reactive carbons, preferentially reacting with the nitrogen site. In the same way, the formation of a pyridine-like moiety again may start from the inclusion of a —CH=N— group within a broken adjacent phenyl ring.

It is interesting to recall that the formation of tertiary amines is not favored in particle bombardment processes (see Figure 4b), suggesting that random fragmentations like those expected in particle bombardment do not prompt the formation of tertiary amines. The mechanisms of formation of such complex products are a matter for further investigation, belonging to the relatively undefined field of "char" formation reactions in pyrolysis studies.

Beyond the classes of reactions involving the modification of the chemical state of N, we have to take into account also the class of reactions producing the depletion of N. It is noted that the depletion of nitrogen is delayed with respect to its modification, the starting fluence corresponding respectively to a fluence or to a temperature where most of the initial imidic nitrogen has been transformed into other functional forms. Hence, the reaction proceeds as it needs to be prompted by the transformation in a suitable precursor for the formation of a volatile species. We propose such a precursor is the nitrile group, which is easily formed according to Scheme II as a product of the decarbonylation process. The related volatile species is proposed to be HCN or the CN^- anion, according to literature results for thermal degradation of polyimides[32] and to recent SIMS reports on the ion-induced fragmentation pattern of PMDA–ODA.[39] SIMS results also show the presence of the fragment CNO^- in bombarded PMDA–ODA, again in agreement with Scheme II of reaction.

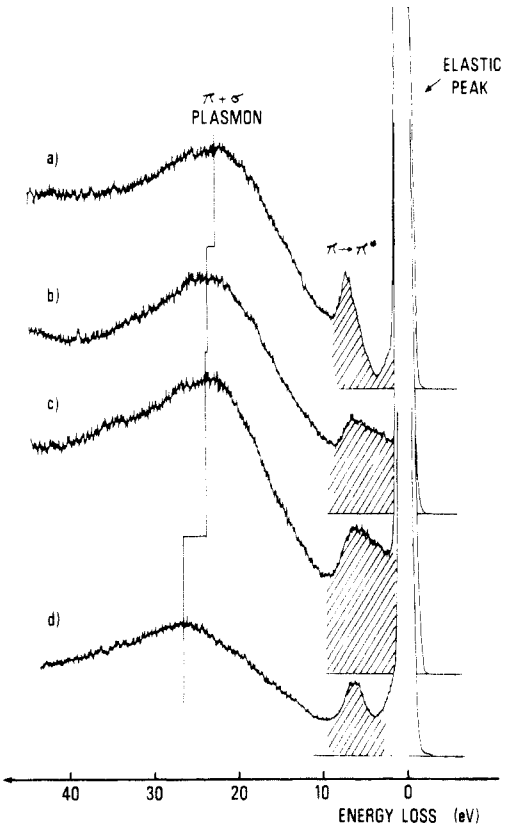

Figure 5. REELS spectra of (a) virgin PMDA–ODA; (b) PMDA–ODA heated for 1 h at 600 °C; (c) PMDA–ODA heated for 3 h at 600 °C; (d) pyrolytic graphite. The energy of the primary electron beam was 1200 eV.

(4) Reflection Electron Energy Loss Spectra. The above-reported XPS data allow us to follow the chemical reactions in terms of the change of the chemical state of O- and N-containing groups.

The REELS technique provides a direct insight into the electronic structure of the solid in terms of interband and intraband transitions, involving occupied and empty levels in valence and conduction bands, and collective excitations (surface and bulk plasmons).

Among the various transitions observed in organic and polymeric systems, the $\pi \rightarrow \pi^*$ transitions due to excitations localized in phenyl rings are particularly evident. Therefore, the REELS technique allows control of the integrity of aromatic rings and of the change in the electronic structure of differently treated PMDA–ODA samples.

Figure 5 shows the REELS spectra obtained for respectively virgin and thermally-treated PMDA–ODA surfaces, as well as for a pyrolytic graphite surface. The energy of the primary electron beam was set at 1200 eV in order to have a sampling depth comparable with that of XPS C 1s peaks, obtained with Al Kα radiation, so that the two techniques investigate essentially the same layer. The IMFP of electrons having this kinetic energy in PMDA–ODA has been evaluated to be on the order of 28 Å.[24]

Two main features are observed in the virgin PMDA–ODA: first, the low excitation region from 1 to 8 eV is dominated by a sharp peak, centered at 6.8 eV, due to $\pi \rightarrow \pi^*$ excitation localized in the aromatic rings; second, the high-energy region is dominated by the broad structure of the bulk plasmon, whose maximum is positioned around 22.3 eV.

The thermal treatment at 600 °C for 1 h (Figure 5b) and 3 h (Figure 5c) produces a significant modification of the initial spectrum:

(a) The low-energy excitation region is characterized by the appearance of new states in the band gap of the initial material.

(b) The sharp structure at about 6.8 eV is broadened and shifted respectively to 6.3 eV after 1 h and 5.8 eV after 3 h of treatment.

(c) The bulk plasmon is made asymmetric and progressively shifted from 22.3 eV to respectively 23.4 eV (1 h) and 23.7 eV (3 h).

The observed filling of the initial band gap (point a) indicates that the pyrolyzed phase is characterized by a relatively high density of scattering states in the very low excitation region. This finding must be compared with the characteristic smaller density of scattering states in the same low-energy excitation region for the REELS spectrum of graphite, due to its well-known singularity in the density of states at the Fermi level.[40] Hence, we may explain the high density of scattering states either in terms of the formation of a set of (low-energy) intraband transitions, depending on the formation of a half-filled conduction band, or as due to a set of interband transitions involving defect states produced by pyrolysis in the initial band gap.

The broad structure observed after thermal treatments at 6.3 and 5.8 eV is assigned to a plasmon resonance of the π-electrons. Similar structures have been observed in connection with the appearance of ohmic conductivity in keV bombarded polymers.[14] The excitation energy is lower with respect to π-plasmon in graphite (6.8 eV), suggesting that the resonance involves a system different from graphite. In particular, the shift of this structure toward a lower excitation energy (point b) supports the hypothesis that the increase in the density of the scattering states is due to interband transitions to defect states. It is known that interband transitions induce a lowering of the excitation energy of a plasmon resonance.[41] The rising intensity of the 6.3–5.8 eV peak is diagnostic of the increase of the π-electron density in the pyrolyzed material and can be explained as due to the formation of large aromatic systems, possibly embedded in the amorphous polymer matrix.

The excitation values of bulk plasmons in pyrolyzed samples (respectively 23.4 and 23.7 eV) can be compared with the 26.4 eV measured for pyrolytic graphite and the values reported for hydrogenated amorphous carbons obtained by plasma deposition, ranging between 22.9 and 24.0 eV depending upon their hydrogen content.[42]

The reported data as a whole support the hypothesis that pyrolysis up to a temperature of 600 °C produces characteristic hydrogenated amorphous carbon phases, to be considered as pregraphitic phases, rich of extended condensed aromatic rings, good precursors of the graphitic ordering of the materials obtained at higher temperature.[11,42]

The situation is quite different in particle-bombarded PMDA–ODA. Figure 6 shows REELS spectra of the Ar^0-bombarded surfaces. The primary beam energy is the same as that in Figure 5.

The particle-induced modification of PMDA–ODA includes the monotonic decrease of the intensity of the $\pi \rightarrow \pi^*$ structure, while its position remains constant throughout the bombardment, the filling of the very low excitation energy region, and the shift of the $\pi + \sigma$ bulk plasmon toward increasing energy with increasing fluence. All these effects reproduce previous results from our laboratory obtained for high-energy ion bombardment.[4,8–10,14]

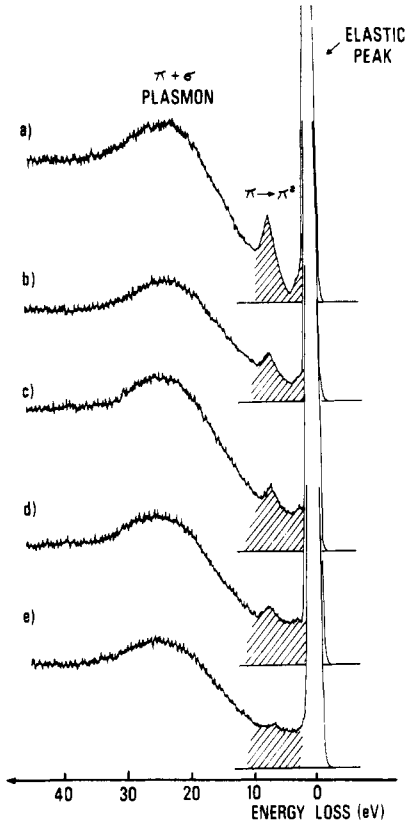

Figure 6. REELS spectra of PMDA–ODA samples bombarded with Ar^0 5 keV: (a) virgin; (b) 4.7×10^{13} Ar^0/cm^2; (c) 2.35×10^{14} Ar^0/cm^2; (d) 9.4×10^{14} Ar^0/cm^2; (e) 1.4×10^{16} Ar^0/cm^2. The energy of the primary electron beam was 1200 eV.

The most relevant feature in particle-bombarded samples consists of the almost complete disappearance of the $\pi \rightarrow \pi^*$ structure, due to the destruction of aromatic rings and in the fact that the π-resonance is not replaced by a new plasmon-like structure as in the case of pyrolyzed samples. This fact strongly suggests that the phases produced by irradiation, in the presently studied fluence range, do not contain more or less extended condensed aromatic systems comparable to those obtained by thermal treatments. The absence of a detectable π-resonance suggests that the bombardment produces highly disordered phases. This picture is supported by the shift observed for the bulk plasmon in bombarded phases from the initial 22.3 eV to 22.8 eV (Figure 6b), 23.6 eV (Figure 6c), 24.8 eV (Figure 6d), and 24.6 eV (Figure 6e). Again these values are in the same range reported for hydrogenated amorphous carbons[42] and far from typical values of 26.5–27.0 eV for graphite.

The obtained amorphous phases are likely rich in radicals and otherwise unsaturated, defective structures, forming a high density of defect states responsible for the filling of the band gap. In fact, such a high density of free electrons and radicals has been observed for the high-energy ion bombardment of PMDA–ODA by ESR measurements.[43,44] Hence, the appearance of electrical conductivity in bombarded samples can be related to the creation of a large density of defect states in the band gap, as an alternative to the formation of extended condensed aromatic systems to explain conductivity.

In order to conclude the comparison between heat-treated and particle-bombarded samples, we note the difference between REELS spectra of pyrolyzed samples in parts b and c of Figure 5, of composition close to that of samples respectively in parts c and d of Figure 6. Again, as above for the chemical structure of samples of close composition, but treated with heat or particle beams, we may conclude that samples of similar compositions have also different electronic structures, depending on the energy deposition way used to produce the compositional modification.

Conclusion

The chemical state of oxygen and nitrogen contained in polyimide has been monitored in order to gain insights into the chemical reactions induced respectively by heat and particle bombardment at low energy.

Compositional data on particle-bombarded and heat-treated samples do not allow us to distinguish between the different processes going on with different intrinsic mechanisms and are not informative of the relevant chemical processes.

Chemical reactions involving the chemical state of oxygen and nitrogen in PMDA–ODA are shown to occur with different rates depending on the method of energy deposition. Furthermore, some specific reactions have been proposed respectively for heat treatment and for particle bombardment.

In summary, thermal treatments proceed essentially through the decarbonylation of imidic rings, which leaves the ether linkage of the PMDA–ODA unit essentially unaffected. This pattern of destruction of the imidic rings is responsible for the transient formation of imine groups which further react in consecutive reactions forming tertiary nitrogen as one of the two main nitrogen products of thermal decomposition, the other one being imine groups included in aromatic rings. It is noteworthy that no imidic nitrogen seems to remain in the pyrolyzed samples. REELS results show that thermal treatment (up to the temperature used in the present work) produces large condensed aromatic systems, embedded in a hydrogenated amorphous carbon phase. Such a biphasic structure, in agreement with results from other authors,[11] can provide a suitable explanation of the conduction properties of pyrolyzed PMDA–ODA.

In the case of particle bombardment, the destruction of imidic rings occurs through different pathways, according to a random mechanism, leaving a detectable concentration of the initial imidic moiety in the irradiated samples. In particular, a specific reaction channel has been identified, involving the production of recoiling oxygen atoms, forming new additional ether or hydroxyl groups with the backbone. Another characteristic irradiation-induced process concerns the simultaneous production of imine and pyridine-like groups, while (at variance with thermal treatments) tertiary nitrogen formation is found to be of negligible intensity. These effects are related to the intrinsic features of the collisional term of energy deposition, i.e., impulse transfer producing reactive recoiling atoms and random fragmentation events. Finally, REELS shows that the electronic structure of the particle-bombarded samples is different from that of the heat-treated samples. In particular, irradiated samples show no evidence of large delocalized aromatic systems observed in the thermal case, while the predominant feature is the filling of the band gap with defect states, related to the formation of highly disordered, radical-rich a-C:H phases.

In general, the particle bombardment induces simultaneous competing processes of backbone reticulation and depletion of fragments containing heteroatoms ("preferential sputtering"). In particular, it should be pointed out that in polymeric targets the "physical" concept of sputtering is no longer suitable, because the emission of gaseous molecules or fragments is not governed by mass

or impact angle (as in physical sputtering) but rather by the stability of the products or the availability of a suitable reaction pathway (chemical sputtering).

The cross-linking reactions produce the densification of the polymer matrix and the formation of a complex hydrogenated amorphous carbon phase. These effects seem qualitatively predominating on the sputtering effects, as is demonstrated by quantitative data reported in the present paper. This result is in agreement with previous RBS measurements showing that in fact the densification process is accompanied by negligible losses of material in ion-irradiated polyimides up to 10^{16} ions/cm^2.[45]

Finally, we remark that previously proposed models of the beam-induced modification of polymers as due to the accumulation of completely graphitized tracks seem inadequate to explain the "mild" and "slow" chemical evolution of the polymeric matrices reported in this paper for low-energy particles as well as for ion beams up to 200 keV as reported in previous papers.[2,4,8-10,14]

Acknowledgment. We thank Prof. S. Pignataro for helpful discussions. MURST (Rome), CNR (Rome), MTA, and OMFB (Budapest) are acknowledged for financial support.

References and Notes

(1) Brown, W. L. *Nucl. Instrum. Methods B* **1989**, *37/38*, 270.
(2) Marletta, G. *Nucl. Instrum. Methods B* **1990**, *46*, 295.
(3) Venkatesan, T.; Calcagno, L.; Elman, B. S.; Foti, G. In *Ion Beam Modification of Insulators*; Mazzoldi, P., Arnold, G. W., Eds.; Elsevier: Amsterdam, The Netherlands, 1987; pp 301–379.
(4) Pignataro, S.; Marletta, G. In *Metallized Plastics 2*; Mittal, K. L., Ed.; Plenum Press: New York, 1991; p 269.
(5) Puglisi, O. *Mater. Sci. Eng.* **1989**, *B2*, 167.
(6) Hioki, T.; Noda, S.; Sugiura, M.; Kakeno, M.; Yamada, K.; Kawamoto, J. *Appl. Phys. Lett.* **1983**, *43*, 30.
(7) Davenas, J.; Xu, X. L.; Boiteux, G. *Synth. Met.* **1988**, *24*, 81.
(8) Marletta, G.; Licciardello, A.; Calcagno, L.; Foti, G. *Nucl. Instrum. Methods B* **1989**, *37/38*, 712.
(9) Marletta, G.; Catalano, S. M.; Pignataro, S. *Surf. Interface Anal.* **1990**, *16*, 407.
(10) Iacona, F.; Marletta, G. *Nucl. Instrum. Methods B* **1992**, *65*, 501.
(11) (a) Hu, C. Z.; Andrade, J. D. *J. Appl. Polym. Sci.* **1985**, *30*, 4409. (b) Hu, C. Z.; De Vries, K. L.; Andrade, J. D. *Polymer* **1987**, *28*, 663.
(12) Toth, A.; Bertoti, I.; Szekely, T.; Sazanov, J. N.; Antonova, T. A.; Shchukarev, A. V.; Gribanov, A. V. *Surf. Interface Anal.* **1986**, *8*, 261.
(13) Anderson, S. G.; Meyer, H. M., III; Atanasoska, L.; Weaver, J. H. *J. Vac. Sci. Technol.* **1988**, *A6*, 38.
(14) (a) Marletta, G.; Oliveri, C.; Ferla, G.; Pignataro, S. *Surf. Interface Anal.* **1988**, *12*, 447. (b) Marletta, G.; Pignataro, S.; Oliveri, C. *Nucl. Instrum. Methods B* **1989**, *39*, 792. (c) Marletta, G.; Pignataro, S.; Oliveri, C. *Nucl. Instrum. Methods B* **1989**, *39*, 773.
(15) Yoshida, K.; Iwaki, M. *Nucl. Instrum. Methods B* **1987**, *19/20*, 878.
(16) Loh, I. H.; Oliver, R. W.; Sioshansi, P. *Nucl. Instrum. Methods B* **1988**, *34*, 337.
(17) Contarini, S.; Schultz, J. A.; Tachi, S.; Jo, Y. S.; Rabalais, J. W. *Appl. Surf. Sci.* **1987**, *28*, 291.
(18) Karpuzov, D.; Kostov, K. L.; Venkova, E.; Kirova, P.; Katardjiev, J.; Carter, G. *Nucl. Instrum. Methods B* **1989**, *39*, 787.
(19) Davenas, J.; Boiteux, G.; Adem, E. H.; Sillion, B. *Synth. Met.* **1990**, *35*, 195.
(20) Matienzo, J.; Emmi, F.; Van Hart, D. C.; Gall, T. P. *J. Vac. Sci. Technol.* **1989**, *A7*, 1784.
(21) Bachman, B. J.; Vasile, M. J. *J. Vac. Sci. Technol.* **1989**, *A7*, 2709.
(22) Flitsch, R.; Shih, D.-Y. *J. Vac. Sci. Technol.* **1990**, *A8*, 2376.
(23) Magnuson, G. D.; Carlston, C. E. *Phys. Rev.* **1963**, *129*, 2403.
(24) Arakawa, E. T.; Williams, M. W.; Ashley, J. C.; Painter, L. R. *J. Appl. Phys.* **1981**, *52*, 3579.
(25) Biersack, J. P. In *Ion Beam Modification of Insulators*; Mazzoldi, P., Arnold, G. W., Eds.; Elsevier: Amsterdam, The Netherlands, 1987; pp 648–740.
(26) Lopez, G. P.; Castner, D. G.; Ratner, B. D. *Surf. Interface Anal.* **1991**, *17*, 267.
(27) Briggs, D. *Polymer* **1984**, *25*, 1379.
(28) Leary, H. J.; Campbell, D. S. *Surf. Interface Anal.* **1979**, *1*, 75.
(29) Buchwalter, P. L.; Baise, A. I. In *Polyimides: Synthesis, Characterization and Applications*; K. L., Mittal, Ed.; Vol. 1, Plenum Press: New York, 1984; p 537.
(30) Iacona, F.; Garilli, M.; Marletta, G.; Puglisi, O.; Pignataro, S. *J. Mater. Res.* **1991**, *6*, 861.
(31) Montaudo, G.; Puglisi, C. In *Development in Polymer Degradation. 7*; Grassie, N., Ed.; Elsevier Applied Science: London, 1987; Chapter 2, pp 35–80.
(32) Jellinek, H. H. G.; Dunkle, S. R. In *Degradation and Stabilization of Polymers*; Jellinek, H. H. G., Ed.; Elsevier: Amsterdam, The Netherlands, 1983; pp 66–161.
(33) Wagner, C. D.; Riggs, W. M.; Davis, L. E.; Moulder, J. F.; Mullenberg, G. E. *Handbook of X-Ray Photoelectron Spectroscopy*; Perkin-Elmer Corp.: Eden Prairie (U.S.A.), 1978.
(34) Pireaux, J. J.; Riga, J.; Boulanger, P.; Snauwaert, P.; Novis, Y.; Chtaib, M.; Gregoire, C.; Fally, F.; Beelen, E.; Caudano, R.; Verbist, J. *J. Electron Spectrosc. Relat. Phenom.* **1990**, *52*, 423.
(35) Ferl, J. E., Long, E. R., Jr. *IEEE Trans. Nucl. Sci.* **1981**, *NS-28*, 4119.
(36) Paik, K. W.; Ruoff, A. L. *J. Adhes. Sci. Technol.* **1990**, *4*, 465.
(37) Flottman, T.; Lohmann, W. In *Metallized Plastics 2*; Mittal, K. L., Ed.; Plenum Press: New York, 1991; p 97.
(38) Bodo, P.; Sundgren, J.-E. *J. Vac. Sci. Technol.* **1988**, *A4*, 2396.
(39) Eldridge, B. N.; Feger, C.; Goldberg, M. J.; Reuter, W.; Scilla, G. J. *Macromolecules* **1991**, *24*, 3209.
(40) Raether, H. Excitation of Plasmon and Interband Transitions by Electrons. *Springer Tracts in Modern Physics*; Springer: New York, 1979; Vol. 88.
(41) Colliex, C. In *Advances in Optical and Electron Microscopy*; Cosslett, V. E., Barer, R., Eds.; Academic Press: London, 1984; Vol. 9, pp 65–177.
(42) Fink, J.; Muller-Heinzerling, T.; Pfluger, J.; Bubenzer, A.; Koidl, P.; Crecelius, G. *Solid State Commun.* **1983**, *47*, 687.
(43) Noda, S.; Hioki, T. *Carbon* **1984**, *22*, 359.
(44) Davenas, J.; Boiteux, G.; Jardin, C.; Gamoudi, M. *Mol. Cryst. Liq. Cryst.* **1990**, *187*, 249.
(45) Calcagno, L.; Foti, G. *Nucl. Instrum. Methods B* **1987**, *19/20*, 895.

Registry No. PMDA–ODA (copolymer), 25038-81-7; PMDA–ODA (SRU), 25036-53-7; Ar, 7440-37-1.